Using bacterial cell growth to template catalytic asymmetry†

Bryan Kaehr*[a] and C. Jeffrey Brinker[abc]

Received 18th March 2010, Accepted 24th May 2010
First published as an Advance Article on the web 11th June 2010
DOI: 10.1039/c0cc00468e

We report an approach to position gold nanoparticle catalysts for metal reduction asymmetrically on a biological template (*E. coli*) by exploiting the polarity of the bacterial cell envelope undergoing growth and division.

The use of biological structures to template inorganic materials has become an increasingly widespread strategy to develop otherwise synthetically inaccessible hierarchical structures under mild chemical conditions, for use as catalytic and device materials. For example, proteins, peptides, DNA, viruses, cells and multicellular structures have been employed as templates to develop inorganic particles, wires, and optical devices.[1–3] While most of these approaches have treated the biological structure as a static template, the development of strategies to recruit biological processes (*e.g.*, cell growth and differentiation) to direct active templating/positioning would greatly expand the pool of synthetic outcomes and potential applications for a given biotemplate. Here, we report an approach to (1) metalize the bacterial cell envelope and (2) segregate metallic regions by exploiting the polarity of the cell envelope undergoing growth and division. This strategy is applied to the synthesis of asymmetric catalytic micro-particles that are capable of 'bacterial-like' swimming behavior in the presence of chemical fuel.

Fig. 1A describes the approach used to metalize the bacterial cell envelope. Similar to previous work,[4,5] positively charged gold nanoparticles (AuNPs) deposit on the bacterial cell envelope *via* electrostatic interactions with negatively charged moieties [predominantly carboxyl and phosphate groups[6]] located on the cell envelope. In a typical experiment, *E. coli* cells were incubated with AuNP seeds (1.4 nm diameters, see ESI† for experimental details) at a ratio $\sim 10^6$ per bacterial cell for $\sim$20 minutes at room temperature. AuNPs bound to the cell envelope catalyze reduction of aqueous metal ions (*e.g.*, Au^{3+}, Ag^{2+}, Pt^{2+}) in the presence of a reducing agent, leading to particle growth that can be visualized as opaque areas on cells using optical microscopy (Fig. 1B). Thus, autometallographic development of AuNPs indicates their location on the cell surface. Development of AuNPs using Au^{3+} and Pt^{2+} immediately following nanoparticle incubation with stationary phase cells showed AuNP binding occurs

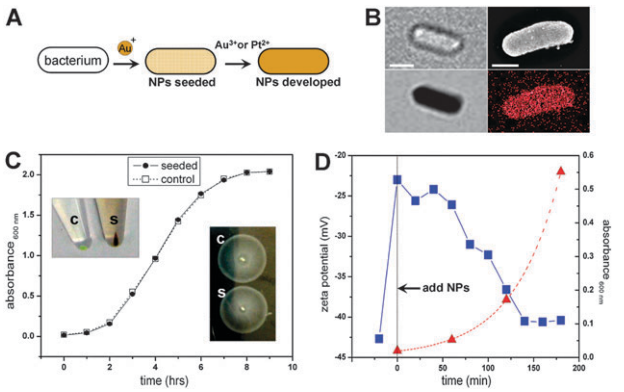

Fig. 1 Biocompatible catalyst seeding and subsequent metallization of bacterial cells. (A) AuNPs bind to the bacterial cell envelope *via* electrostatic interactions. AuNPs catalyze metallization of the cell envelope *via* reduction of solution ions of Au^{3+} or Pt^{2+}. (B; scale bars, 1 μm) Optical microscopy image of an AuNP targeted *E. coli* before (upper left panel) and after (lower left panel) metallization with gold. (Upper right panel) SEM of a platinum metallized bacterium (lower right panel; EDS map of Pt). (C) *E. coli* seeded with AuNPs (labeled, 'S') and recovered *via* centrifugation (left inset) display no significant difference in growth rates and chemotaxis properties (right inset) compared to controls (labeled 'C'). (D) Zeta potential of an *E. coli* population, maintained in growth media, following incubation of AuNPs (blue). Red line shows first 4 points of the 'seeded' exponential growth curve shown in C.

homogenously over the whole cell envelope across the population (>99% of cells) to produce hollow metallic shells (S1, ESI†). X-ray diffraction (XRD) of cell-templated platinum shells showed sharp peaks attributed to face-centered cubic (fcc) platinum particles of *ca.* 5 nm in size (S2, ESI†). Cell-templated gold shells displayed resistivities nearing that of bulk gold, and the length of the wire could be modified using antibiotic treatment (S3, ESI†).

The use of whole cells as templates for inorganic materials produces, in general, structures with relatively larger feature sizes as compared to other studies that have used cell constituents (*e.g.*, DNA, peptides, microtubules, *etc.*) as templates. Yet, employing viable microorganisms to fabricate/template device materials may offer a number of advantages, for instance, to organize a desired functionality on a bio-template by exploiting cell processes (*e.g.*, growth[7]), engineering cell behaviors to achieve desired morphologies[8] as well as to enable the self-assembly of functionalized biotemplates using innate or engineered environmental responses (*e.g.*, chemotaxis of motile cells). These strategies require that aspects of the synthesis must be compatible with cell viability.

Therefore, we investigated the effects of AuNPs bound to the cell envelope on cell behavior. Fig. 1C shows AuNP

[a] *Sandia National Laboratories, Advanced Materials Lab, NM 87106, USA. E-mail: bjkaehr@sandia.gov*
[b] *Center for Micro-Engineered Materials, University of New Mexico, Albuquerque, NM, USA*
[c] *Departments of Chemical and Nuclear Engineering and Molecular Genetics and Microbiology, University of New Mexico, NM, USA*
† Electronic supplementary information (ESI) available: Experimental section, Fig. S1–S4 and supporting movies. See DOI: 10.1039/c0cc00468e

deposition onto *E. coli* does not attenuate normal growth, motility or chemotactic response compared to controls. By monitoring the zeta potential of cells during incubation in nutrient media, attenuation of the negative potential of bare cells (~ -40 mV) by AuNP binding (~ -20 mV) is essentially recovered after ~ 2.5 h corresponding to the onset of log phase growth (Fig. 1D). Cells harvested and AuNPs developed at >3 h show little to no staining across the population (S1, ESI†). However, cells stained at ~ 40–120 min showed heterogeneous coverage over the cell envelope, indicating that cells with bound AuNPs were undergoing growth and not simply being diluted from the developing population.

In order to follow the trajectory of envelope-bound AuNPs on single cells undergoing growth, AuNP seeded cells deposited at a nutrient agarose/glass interface were imaged over time and nanoparticles were developed following growth and formation of the septum. Fig. 2A shows a representative time-lapse sequence of a NP-seeded bacterium and indicates AuNP development, following elongation and septum formation, is confined primarily to the poles of the bacterium (Fig. 2A, panel 4, arrows), a result verified using SEM/EDS analysis of cultures grown for ~ 50–60 min in liquid media (Fig. 2B).

These results are consistent with the current model of *E. coli* sacculus elongation and division.[9–11] Under growth conditions, *E. coli* cells double in size and then divide at the midpoint. Recent work has shown that insertion of new cell envelope material during elongation occurs primarily along the central surface of the cell rod, with the polar caps remaining metabolically inert.[12,13] Backscatter SEMs of AuNPs developed on bacterial templates following one to two rounds of cell replication show that metallic regions can be mapped to the inert pole during the stages of murein segregation in the cell wall (Fig. 2C). These results indicate that AuNPs electrostatically bound to the whole cell envelope, in large part, are diluted or otherwise lost to envelope turnover in the central cell envelope during growth and division, remaining relatively concentrated only at the poles where neither process occurs to a substantial extent.[13]

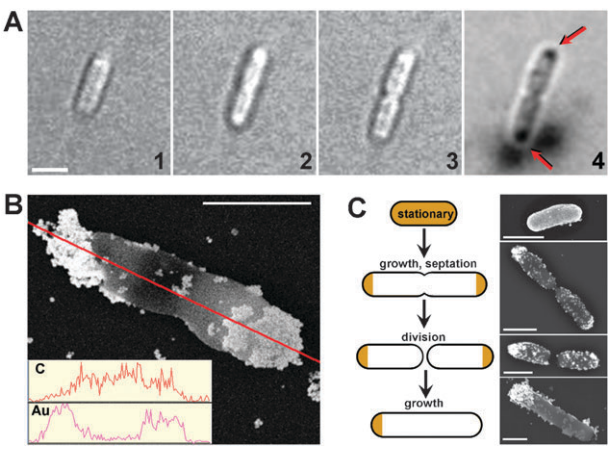

Fig. 2 Analysis of AuNP coverage on single cells following incubation in growth conditions and development with gold solutions. (A) A single *E. coli* seeded with AuNPs (as in Fig. 1B top left panel) was monitored over time (panels 1–4 span ~ 2.5 h at 23 °C). Following formation of the septum (panel 3), the cell was bathed in gold development solution. Panel 4 shows staining was largely confined to the poles of the dividing bacterium (arrows). (B) Backscatter SEM image shows gold deposition following development of AuNPs is primarily confined to the cell poles (B; inset) An energy dispersive X-ray spectrograph (EDS) across the red line shows the carbon trace of the bacterium and the gold trace concentrated at the cell poles. (C) Stages of murein segregation (left, adapted from ref. 13) show that the location of the metabolically inert pole (gold) corresponds to regions of metallization of AuNP seeded cells undergoing growth and division (right, SEM images). Scale bars, 2 μm.

This straightforward approach to segregate catalytic regions on a biotemplate using cell growth provides an alternative route to explore micro/nano-scale device applications that require asymmetric distribution of electrical contacts, electrostatic surface charge, plasmonic and/or catalytic regions using bio-templating (mild, inherently "green") reaction conditions.[3] Applications for asymmetric materials include energy storage, constituents for self-assembly, and nano-propulsion. As an example of the latter, several proposed designs for chemically driven, catalytic nanomotors require asymmetric arrangement of metallic components (*e.g.*, platinum and gold) in order to develop propulsion along forward, orbital and rotational trajectories.[14,15]

We investigated whether *E. coli* cell templates, metallized asymmetrically *via* cell growth, could undergo a second metallization reaction. *E. coli* cells seeded with AuNPs were grown for ~ 60 min and AuNPs were developed with gold solutions (generating Au particle patterns similar to Fig. 2B and C, lower three panels), followed by a second AuNP-incubation. Subsequent development of AuNPs using gold or platinum showed metallization over the whole cell (S4, ESI†), indicating the electrostatic interaction between positively charged AuNPs and nascent cell envelope, formed during growth, was largely unaffected following the first exposure to NP development reagents.

Using platinum as the second metallic component produced outgrowths (ranging in size and position on the particle envelope; S4, ESI†) of high Pt concentration extending asymmetrically from the cell body (Fig. 3A, left panel). Outgrowth formation

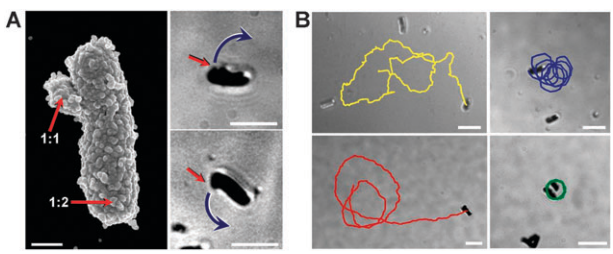

Fig. 3 Motion of Pt–Au microparticles templated from *E. coli*. (A, scale bar 0.5 μm) SEM of a Pt–Au microparticle displaying an outgrowth formed after second metallization step (reduction of Pt). Numbers indicate the atomic weight ratio of Pt : Au measured using an EDS spot (diameter, 500 nm) centered at the arrow point (right panels). Observed motion in 1.0% hydrogen peroxide is in the direction of outgrowths (arrows) corresponding to high Pt concentration (see movie S1, ESI †). (B; scale bars, 5 μm) Left and right turns (upper left panel), small (upper right panel) and large (lower left panel) radii orbital and rotational (lower right panel) trajectories (colored lines) were observed with velocities ranging from 3–6 μm s^{-1}.

was governed, most likely, from the asymmetric distribution of nucleation sites following growth and initial (gold) metallization, as uniform Pt metallization over the cell envelope was observed in the absence of a cell growth step (*e.g.*, Fig. 1B, top right panel).[16] Pt–Au particles were rinsed (H_2O), desiccated (>24 h), and immersed in a solution of 1% H_2O_2. Where nodules on single cells could be resolved, propulsion, due to the Pt catalyzed reaction $2H_2O_2 \rightarrow 2H_2O + O_2$, was observed in the direction of nodule outgrowth (Fig. 3A, right panels), corresponding to high Pt concentration and consistent with previous observations and proposed mechanisms of bi-segmented Pt–Au particle motility.[14] Further, particles undergoing left and right turns (Fig. 3B, upper left panel), small (upper right panel) and large (lower left panel) radii orbital and rotational (lower right panel) trajectories were observed (Fig. 3B) with velocities ranging from 3–6 μm s^{-1} (see movies S1–S4, ESI†). Segmentation of gold and platinum regions across the cell rod could not be definitively resolved using EDS. However, nodule outgrowth and motility of particles comprised of single bacteria was not observed when sequential metallization (gold followed by platinum) was not interceded by a cell growth step, indicating metallic asymmetry—achieved here using cell growth—was needed for directional movement. More uniform bimetallization should be achievable by employing synchronous cultures[17] coupled to density or electrostatic separation strategies following cell growth, and navigation of motile particles by external control can be accomplished, for instance, by incorporation of ferromagnetic components (*e.g.*, nickel) during metallization.

In summary, we have shown that segregation of catalytic regions on a biotemplate can be achieved by exploiting the polar development of *E. coli* cells undergoing growth and division. These results provide a foundation to further investigate dynamic bio-templating using other cell types and cell-cycle dependent behaviors (*e.g.*, sporulation, pili/flagella expression) and develop more complex materials and architectures using chemical, genetic, and confinement-induced modification of bacterial morphology[8] and surface properties.[18]

We thank Constantine Khripin and Darren Dunphy for useful discussions. We acknowledge the U. S. DOE Office of Basic Energy Sciences and AFOSR grant FA 9550-07-1-0054 for support. BK gratefully acknowledges the Sandia National Laboratories Truman Fellowship in National Security Science and Engineering and the Laboratory Directed Research and Development program for support. This work was performed, in part, at the Center for Integrated Nanotechnologies, a U. S. DOE user facility at Los Alamos National Laboratory (Contract DE-AC52-06NA25396) and Sandia National Laboratories. Sandia is a multiprogram laboratory operated by Sandia Corporation, a Lockheed Martin Company, for the United States DOE's NNSA under Contract DE-AC04-94AL85000.

Notes and references

1 S. Sotiropoulou, Y. Sierra-Sastre, S. S. Mark and C. A. Batt, *Chem. Mater.*, 2008, **20**, 821–834.
2 N. Ma, E. Sargent and S. Kelley, *J. Mater. Chem.*, 2008, **18**, 954–964.
3 M. Dickerson, K. Sandhage and R. Naik, *Chem. Rev.*, 2008, **108**, 4935–4978.
4 V. Berry and R. F. Saraf, *Angew. Chem., Int. Ed.*, 2005, **44**, 6668–6673.
5 V. Berry, A. Gole, S. Kundu, C. Murphy and R. Saraf, *J. Am. Chem. Soc.*, 2005, **127**, 17600.
6 F. Ferris and T. Beveridge, *Can. J. Microbiol.*, 1986, **32**, 52.
7 Z. Li, S. Chung, J. Nam, D. Ginger and C. Mirkin, *Angew. Chem. Int. Ed.*, 2003, **42**, 2306–2309.
8 S. Takeuchi, W. DiLuzio, D. Weibel and G. Whitesides, *Nano Lett.*, 2005, **5**, 1819.
9 M. Cabeen and C. Jacobs-Wagner, *Nat. Rev. Microbiol.*, 2005, **3**, 601–610.
10 D. Scheffers and M. Pinho, *Microbiol. Mol. Biol. Rev.*, 2005, **69**, 585.
11 E. Stewart, R. Madden, G. Paul and F. Taddei, *PLoS Biol.*, 2005, **3**, e45.
12 A. Koch and C. Woldringh, *J. Theor. Biol.*, 1994, **171**, 415–425.
13 M. De Pedro, J. Quintela, J. Holtje and H. Schwarz, *J. Bacteriol.*, 1997, **179**, 2823.
14 W. Paxton, S. Sundararajan, T. Mallouk and A. Sen, *Angew. Chem., Int. Ed.*, 2006, **45**, 5420–5429.
15 J. Wang, *ACS Nano*, 2009, **3**, 4–9.
16 No structure directing agents (SDAs; *e.g.*, polymer capping agents, surfactants, *etc.*) were used to control morphology of Pt outgrowths. Use of SDAs, in conjunction with the dynamic bio-templating approach presented here and over a range of incubation times for metallization should enable more precise control over the morphology and ratio of incorporated metals.
17 D. Bates, J. Epstein, E. Boye, K. Fahrner, H. Berg and N. Kleckner, *Mol.Microbiol.*, 2005, **57**, 380–391.
18 P. Curnow, P. Bessette, D. Kisailus, M. Murr, P. Daugherty and D. Morse, *J. Am. Chem. Soc.*, 2005, **127**, 15749–15755.

